

A. E. Bulyshev, N. V. Denisova, N. G. Preobrazhenskii,  
and A. E. Suvorov

UDC 533.9.01

Electrodeless high-frequency (HF) discharges are widely used in physics, particularly because they provide good line-emission sources [1, 2]. They have recently been used in optogalvanic experiments [3, 4]. It is therefore important to construct a correct model for an HF discharge plasma. Some steps in that direction have been described in [5, 6], where Schottky's diffusion model was used in a numerical method for determining an electromagnetic field, where it was shown that the skin effect is appreciable. However, a self-consistent solution was not given in [5, 6], i.e., the plasma and electromagnetic-field parameters were not determined together. A long series of calculations has been performed [7] on electrodeless high-frequency lamps (see also bibliography there), and the temperatures and populations have been determined for plasma components, particularly mixtures of inert gases and metal vapors in low-power discharges with minor skin-layer effects. The electromagnetic fields were not calculated, while the energy balance was incorporated in a simple fashion.

Here we give a method of constructing a self-consistent solution for the plasma-field system in an electrodeless HF discharge; it is designed for plasma parameters when the skin effect is prominent, and a computational procedure is given for the spatial distribution and field strengths. Estimates are made to determine how the deposited energy, mean electron concentration, and mean electron temperature are dependent on the external field, gas type, and geometrical factors. Detailed calculations are made for a discharge in argon.

1. The discharge burns in a tube and is represented as an unbounded cylinder, radius R, placed in a solenoid. The plasma is considered as homogeneous along the axis, and all the parameters are dependent only on the radial coordinate. An ambipolar-diffusion model is used, as in [5-7]. A Maxwellllan electron-energy distribution was assumed, with  $T_e$  constant over the cross section, because the electron thermal conductivity is high at low gas pressures ( $p \approx 10^3$  Pa [8]). Electron-ion recombination occurs at the walls. We neglect bulk recombination.

The equations are

$$\begin{aligned} \partial n_e / \partial t &= D_a \Delta n_e + S_e n_e, \\ \partial \left( \frac{3}{2} n_e T_e \right) / \partial t &= - \operatorname{div} q + S^+ - S^-, \quad \operatorname{rot} \mathbf{H} = 4\pi\sigma \mathbf{E}/c, \\ \operatorname{rot} \mathbf{E} &= -i\omega \mathbf{H}/c, \quad \operatorname{div} \mathbf{E} = 0, \quad \operatorname{div} \mathbf{H} = 0, \\ \partial N_k / \partial t &= -A_k N_k + \widehat{H}_k N_k - N_k \sum_i w_{ki} + \sum_i w_{ik} N_i - \gamma_k N_k. \end{aligned} \tag{1.1}$$

Here  $n_e$  is electron concentration;  $D_a$ , ambipolar diffusion coefficient;  $S_e$ , electron generation rate constant consequent on collisional ionization;  $T_e$ , electron temperature;  $q$ , electron energy flux;  $S^+$  and  $S^-$ , source and sink terms in the energy equation;  $\mathbf{H}$  and  $\mathbf{E}$ , magnetic and electric field amplitudes, which are related to the external HF field;  $\sigma$ , complex conductivity at the field frequency;  $N_k$ , the population in excited state  $k$ ;  $A_k$ , radiative damping constant for level  $k$ ;  $\widehat{H}_k$ , Holstein operator [10];  $w_{ki}$ , rate constant for collisional transition from level  $k$  to level  $i$ ; and  $\gamma_k$ , ionization rate constant. The coefficients in (1.1) are

$$\begin{aligned} S_e &= \sum_{h=1}^{\infty} N_h \langle \sigma_h v \rangle \exp(-I_h/T_e), \\ S^- &= \sum_{h=2}^{\infty} \sum_{n < h} E_{hn} N_n n_e \langle \sigma_{nh} v \rangle \exp(-E_{hn}/T_e) \end{aligned}$$

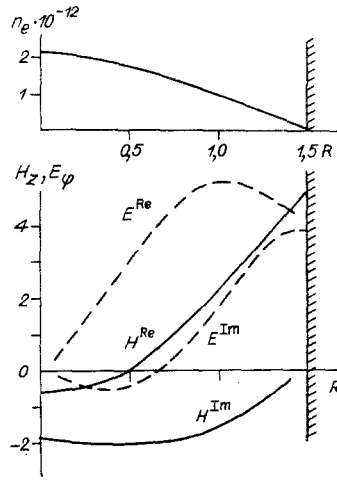


Fig. 1

$$S^+ = \langle jE \rangle + \sum_{h=1}^{\infty} \sum_{n>k} E_{kn} N_n n_e \langle \sigma_{nh\nu} \rangle, \quad \sigma = n_e e^2 (\gamma - i\omega) / m_e (\gamma^2 + \omega^2), \quad (1.2)$$

where  $\sigma_k$  is the ionization cross section for level  $k$ ;  $E_{kn}$ , energy of the transition between levels  $k$  and  $n$ ;  $I_k$ , corresponding ionization potential;  $\sigma_{nk}$ , cross section for collisional transition from level  $n$  to level  $k$ ;  $j_e$  and  $E_a$ , current density and electric field due to ambipolar diffusion;  $j$  and  $E$ , current density and field at  $\omega = 1$  MHz; and  $\gamma$ , electron-ion elastic-collision frequency. System (1.1) is supplemented with the boundary conditions

$$n_e(R) = 0, \quad \partial n_e / \partial r|_{r=0} = 0, \quad H|_{r=R} = H_0, \quad \partial H / \partial r|_{r=0} = 0, \quad E|_{r=0} = 0.$$

The magnetic-field vector contains only a  $z$  component ( $z$  along the cylinder axis), and the electric field has only an azimuthal component. Before we solve (1.1), we make some estimates that subsequently give a clearer understanding of how the absorbed power is dependent on the discharge parameters.

2. If there is a skin layer, thickness  $\ell < R$ , the energy dissipation rate is [9]

$$Q = \int_V S^+ dV \sim C_1 H_0^2 / \sqrt{\bar{n}_e} \quad (2.1)$$

( $C_1$  is a constant, while  $\bar{n}_e$  is the characteristic electron concentration). The total energy loss  $P = \int_V S^- dV$  is linearly dependent on  $\bar{n}_e$  if this is not too large, so  $P \sim C_2 \bar{n}_e$  and we

solve  $Q = P$  to get

$$\bar{n}_e \sim C_3 H_0^{4/3}, \quad (2.2)$$

$$Q \sim C_4 H_0^{4/3}. \quad (2.3)$$

One can draw certain conclusions on the stability when there is a skin layer. If the electron concentration fluctuates upwards, that layer thins, and the temperature falls, which reduces the electron source, and  $n_e$  falls by diffusion. The plasma-field system therefore has a stability margin.

It is virtually impossible to solve (1.1) analytically in the general case, so we examine model equations for minor deviations from equilibrium in the plasma parameters. Let  $\bar{n}_e$  and  $\bar{T}_e$  be the electron concentration and temperature averaged over the volume, with energy production  $Q \sim C_5 / \sqrt{\bar{n}_e}$ , and diffusion incorporated via the diffusion time  $\tau_a$ . Then we have the linearized equations

$$dn'_e/dt = -n'_e/\tau_a + AT'_e, \quad dT'_e/dt = -Bn'_e, \quad (2.4)$$

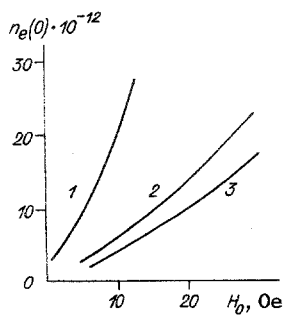


Fig. 2

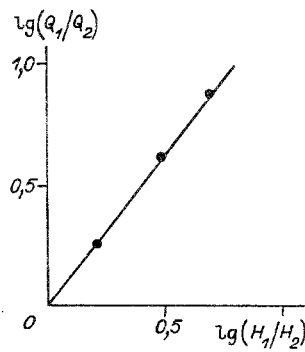


Fig. 3

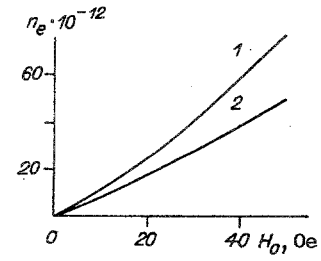


Fig. 4

where  $n_e'$  and  $T_e'$  are the deviations of  $\bar{n}_e$  and  $\bar{T}_e$  from the stationary values and  $A = (\partial S_e / \partial T) \bar{n}_e$ ;  $B = |\partial Q / \partial n_e|$ .

If  $1/(2\tau_a)^2 - AB \geq 0$ , (2.4) has a purely damped solution, but otherwise there is an oscillating component having frequency  $\omega = \sqrt{AB - 1/(2\tau_a)^2}$ . The oscillation mechanism is in effect described above, while the damping is due to dissipation.

3. Two forms of numerical solution have been devised. The first is based on the Schottky model (original or modified), while the second involves solving (1.1) directly. In the first, we calculated also the discharge parameters (weak fields  $H_0$ , low  $n_e$ ), when ionization is from the ground state on Schottky's assumption. Then we get a stationary solution for the ambipolar diffusion equation  $n_e(r) = n_e(0)J_0(\xi r)$  ( $\xi = \sqrt{S_e/D_a}$ ,  $J_0(\xi r)$  is a zero-order Bessel function). The boundary condition  $n_e(R) = 0$  gives an equation for the temperature:

$$\xi R = 2.405. \quad (3.1)$$

These arguments are taken from Schottky's theory. To determine  $n_e(0)$ , we used a stationary equation involving integration over the volume for the energy balance,  $\int_V (S^+ - S^-) dV = 0$ , with

the integrals derived by Simpson's method in the numerical calculations. The source term  $S^+$  requires a knowledge of the electric field  $E_\varphi$ , where we used the skin-layer equation for  $H_z$  and Maxwell's equation for  $E_\varphi$ :

$$\Delta H_z - iH_z/l^2 = 0, \quad \text{rot } H_z = 4\pi\sigma E_\varphi/c, \quad (3.2)$$

where  $l$  is the skin-layer thickness and  $\Delta$  is the Laplace operator in a cylindrical coordinate system; (3.2) was approximated on a difference grid along the radius with second-order accuracy. The finite-difference equation was solved by matrix fitting.

Figure 1 shows calculations on  $n_e(r)$  together with the  $H_z$  and  $E_\varphi$  profiles for  $H_0 = 5$  Oe and  $N_0 = 10^{15} \text{ cm}^{-3}$  ( $N_0$  atomic concentration, with  $H^{\text{Re}}$  and  $E^{\text{Re}}$  the real field components, while  $H^{\text{Im}}$  and  $E^{\text{Im}}$  are the imaginary ones). Tube radius  $R = 1.5$  cm, electron temperature corresponding to these parameters  $T_e = 2.7$  eV, and  $H_z$  and  $E_\varphi$  given in cgs units.

Several calculations were performed to examine the dependence of  $n_e$  and  $T_e$  on  $N_0$  and the external field amplitude. Figure 2 shows lines 1-3 corresponding to  $N_0 = 5 \cdot 10^{15}$ ;  $10^{15}$ ;  $7 \cdot 10^{14} \text{ cm}^{-3}$  and  $T_e = 1.7, 2.7, 3$  eV, where it is evident that  $T_e$  is independent of  $H_0$  (as Schottky's model implies) but decreases as  $N_0$  increases. The electron concentration increases with  $H_0$  and  $N_0$ . There is satisfactory agreement with (2.2). The numerical calculations also confirm (2.1) and (2.3), and Fig. 3 compares (2.3) with the calculations: the straight line is from (2.3) and the points are from numerical calculation.

The modified Schottky model has recently been widely used [13], which incorporates ionization from excited levels, but it is assumed that  $S_e = \sum_i S_{ei}$  is only slightly dependent

on the coordinates, so the entire Schottky-model formalism can be retained. The populations are calculated from the kinetic equation in (1.1). The inelastic cross sections were taken in the Dravin approximation [10]. The Biberman factor [10] was used to correct for radiation diffusion in the resonant transitions, while the oscillator strengths were taken from [11]. The resonant charge-transfer cross section was taken from [12]. A multilevel model was used for the argon atom [10]. Closely spaced levels were combined in the blocks. Up to 15 blocks were used in the detailed calculations. Levels above the sixth were considered as hydrogen-like [10]. The second calculation method involved solving (1.1) directly. The temperature

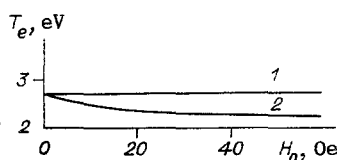


Fig. 5

was taken as constant over the volume and determined from the integral energy equation. The electron concentration was calculated from the nonstationary ambipolar-diffusion equation by the pivot method. An important point concerns the choice of number of level blocks. We chose the number with a safety margin in order that the addition of new levels would not affect the ionization-rate calculation.

Figure 4 shows the electron concentration at the center of the tube,  $R = 1.5$  cm, as a function of  $H_0$  ( $N_0 = 10^{15}$  cm $^{-3}$ , 1 and 2 from the modified Schottky model and the original). There was almost exact coincidence from the complete scheme and the modified Schottky theory. Figure 5 compares temperatures (1 from the Schottky model, 2 from the complete scheme and the modified theory). The Schottky model becomes incorrect at sufficiently high  $H_0$ . In strong fields ( $H_0 \sim 100$  Oe) with  $N_0 = 10^{15}$  cm $^{-3}$ , there was agreement between the calculations for 10-level and two-level models, so in weak fields ( $H_0 \leq 10$  Oe), the Schottky model applies, and it is sufficient to take a single level, while at high fields, there is ionization from the first excited level (the instantaneous-ionization model applies [10]), and it is sufficient to take two levels. This is confirmed by the temperature calculations (Fig. 5). At high  $H_0$ , the  $T_e(H_0)$  curve tends to a constant coincident with the solution in the Schottky model provided that the ionization potential is taken as the excitation energy for the first level, which means that the instantaneous-ionization approximation applies there.

In conclusion, we consider estimates for processes neglected in our model. Let  $P = P_1 + P_2 + P_3$ , where  $P_1$  is the loss in exciting atoms to the resonant level,  $P_2$  that in elastic collisions, and  $P_3$  that due to electrons reaching the wall. All of these were calculated per

unit length. Then  $P_1 = \int_V E_1 \langle \sigma_n v \rangle \exp(-E_1/T_e) N_0 n_e dV \sim E_1 \sigma_n \bar{v} N_0 \bar{n}_e \exp(-E_1/T_e) R^2$  ( $E_1$  is the excitation potential for the first level,  $\sigma_n$  the excitation cross section, and  $\bar{v}$  the mean electron speed),  $P_2 = \int T_e \langle \sigma_e v \rangle N_0 n_e 2m_e dV/M \sim T_e \sigma_e \bar{v} N_0 n_e R^2 m_e/M$  ( $\sigma_e$  the elastic scattering cross section and  $M$  atomic mass),  $P_3 = \int T_e j_e dS \sim T_e D_a \nabla n_e R \sim T_e D_e n_e D_a/D_e$  ( $j_e$  electron flux to the wall,  $D_a$  and  $D_e$  ambipolar and electron diffusion coefficients, with integration over the surface of the cylinder), and  $P_2/P_1 \sim T_e \exp(E_1/T_e) m_e/(E_1 M)$ ,  $P_3/P_1 \sim T_e \exp(E_1/T_e) \lambda^2 D_a/(E_1 R^2 D_e)$  ( $\lambda$  is the electron mean free path). When the characteristic values are inserted, the contributions from  $P_2$  and  $P_3$  do not exceed 1%.

#### LITERATURE CITED

1. É. K. Kraulinya and V. A. Kruglevskii, "Excitation-transfer cross sections in metal-vapor sensitized fluorescence," in: Sensitized Metal-Vapor Fluorescence [in Russian], Latv. Univ., Riga (1977).
2. K. Kuramochi, T. Matsuo, et al., "Special profiles of the  $^{87}\text{RbD}_1$  line emitted from a spherical lamp," Jpn. J. Appl. Phys., 16, No. 5 (1977).
3. T. Suzuki and M. Kakimoto, "High-resolution optogalvanic study of the  $C_4(0)^1\Pi_u, C'_5(0)^1\Sigma_u^+$  and  $a''(0)^1\Sigma_g^+$  Rydberg states of  $\text{N}_2$ ," J. Molecular Spectrosc., 93, 423 (1982).
4. T. Suzuki, "Optogalvanic spectroscopy with RF discharge," Opt. Commun., 28, No. 5 (1981).
5. B. B. Henriksen, D. R. Keefer, and M. N. Clarkson, "Electromagnetic field in electrodeless discharge," J. Appl. Phys., 42, No. 13 (1971).
6. D. R. Keefer, A Theory for the Low-Pressure Electrodeless Discharge, AIAA Paper No. 703, New York (1969).
7. A. S. Agapov, A. A. Matveev, and V. I. Khutorshchikov, "Methods of calculating high-frequency electrodeless-lamp parameters," in: Energy Transfer in Metal Vapors [in Russian], Latv. Univ., Riga (1985).
8. V. L. Granovskii, Electric Currents in Gases [in Russian], Nauka, Moscow (1971).

9. A. E. Bulyshev and N. G. Preobrazhenskii, "Impedance response in an electrodeless HF discharge to optical excitation," Dokl. Akad. Nauk SSSR, 279, No. 6 (1984).
10. L. M. Biberman, V. S. Vorob'ev, and I. T. Yakubov, Nonequilibrium Low-Temperature Plasma Kinetics [in Russian], Nauka, Moscow (1982).
11. W. L. Wiese, M. W. Smith, and B. M. Glennon, "Atomic transition probabilities," NSRDS-NBS, Vol. 4 (1966).
12. J. Hasted, Atomic-Collision Physics [Russian translation], Mir, Moscow (1965).
13. N. K. Zaitsev and N. Ya. Shaparev, Plasma Optoelectric Phenomena [in Russian], Preprint No. 207-209 F, IF SO AN SSSR, Krasnoyarsk (1982).

## MOLECULAR-GAS COOLING IN A RESONANT RADIATION FIELD WITH LINE OVERLAP

A. M. Starik

UDC 533.011+536.14

Recently, there has been much interest in processes where resonant radiation acts on absorbing or amplifying gas media. The changes in macroscopic parameters (temperature or density) are very important, as they govern the refractive-index changes in the beam. In [1-4], molecular-gas cooling mechanisms on absorption were examined, where the frequency is in resonance with the line center of an absorbing vibrational-rotational transition. This kinetic-cooling intermode transition  $00^0_1 \rightarrow 10^0_0$ , wavelength  $\lambda = 10.6 \mu\text{m}$  [5], and in  $\text{CD}_4$  on absorption in the P branch of a vibrational-rotational transition belonging to the  $\nu_4$  mode [6]. The absorption is considered for a solitary spectral line in the absence of overlap with adjacent ones. However, adjacent lines often overlap. The paper discusses molecular-gas cooling mechanisms on light absorption or amplification under these conditions.

Let the gas molecules be rigid rotors, while the frequency  $\nu_I$  in the beam is almost in resonance with the center frequency  $\nu_0$  or the line for a certain vibrational-rotational transition  $m(V', j') \rightleftharpoons n(V'', j'')$ :

$$\nu_I = \frac{E_{V''} - E_{V'} + E_{j''} - E_{j'}}{h} + \Delta\nu \quad (1)$$

Here  $E_{V'}$  and  $E_{V''}$  are the vibrational energies of the lower state  $m$  and upper state  $n$  in the absorbing (amplifying) transition,  $E_{j'}$  and  $E_{j''}$  are the rotational energies there,  $h$  is Planck's constant, and  $\Delta\nu$  is the frequency difference.

We neglect thermal conduction and convection (our characteristic times are substantially less than the ones for those processes), and write the equation describing the temperature as

$$\frac{5}{2} \frac{R}{\mu} \rho \frac{dT}{dt} = J, \quad J = k_\nu I - \frac{de_r}{dt} - \frac{de_v}{dt} \quad (2)$$

where  $T$  is the translational temperature;  $\rho$ , density;  $\mu$ , molecular weight;  $e_v$  and  $e_r$ , vibrational and rotational energies in unit volume;  $k_\nu$ , absorption coefficient; and  $I$ , intensity.

Let the induced-transition time  $\tau_I$  be substantially longer than the polarization relaxation time  $\tau$ . We neglect spontaneous decay and derive the changes in the numbers of molecules in the states  $(V', j')$  and  $(V'', j'')$  that intersect with the radiation from [7, 8]

$$\frac{dN_{j'}}{dt} = -\frac{k_\nu I}{h\nu_I} + J_{RR}^{j'} + J_{RT}^{j'} \quad (3)$$

$$\frac{dN_{j''}}{dt} = \frac{k_\nu I}{h\nu_I} + J_{RR}^{j''} + J_{RT}^{j''} \quad (4)$$